Materials Science & Engineering A 648 (2015) 260–264

Contents lists available at ScienceDirect

Materials Science & Engineering A

journal homepage: www.elsevier.com/locate/msea

Plastic deformation and phase transformations in austenitic steels in the course of hydrogen charging and subsequent mechanical tests

G.S. Mogilny, S.M. Teus, V.N. Shyvanyuk, V.G. Gavriljuk*

G.V. Kurdymov Institute for Metal Physics, Kiev 03680, Ukraine

ARTICLE INFO

Article history:
Received 18 May 2015
Received in revised form
29 July 2015
Accepted 2 September 2015
Available online 8 September 2015

Keywords:
Austenitic steel
Hydrogen embrittlement
Plastic deformation
Crystallographic texrure
$\gamma \rightarrow \varepsilon$ Transformation
Trip effect.

ABSTRACT

This study aims to shed light on some uncertainty in the effect of hydrogen-induced ε-martensite on mechanical behavior of hydrogen charged austenitic steels. It is shown that cathodic charging of austenitic steels is accompanied by plastic deformation, which creates the crystallographic texture and decreases plasticity during subsequent tensile tests. This deformation is the main reason for the hydrogen-induced $\gamma \rightarrow \varepsilon$ transformation. The ε-martensite is formed in the hydrogen-rich areas of the austenite, which decreases the hydrogen content in the retained austenite. In case of a small fraction of the hydrogen-induced ε-martensite, it can be additionally formed during subsequent mechanical tests due to trip effect, which diminishes the hydrogen loss of plasticity.

1. Introduction

Holzworth and Louthan [1] were possibly first to find that hydrogen in a type 304L austenitic steel causes the same martensitic phases, α and ε, as produced by the cold work. Later on, Szummer and Yanko [2], investigating the hydrogen-charged 310 and 304 Cr–Ni steels, detected two phases, fcc and hcp, characterized by about 5% larger lattice parameters as compared with the hydrogen-free austenite and ε-martensite. These phases were denoted as pseudohydrides γ^* and ε^* or γ_H and ε_H. The hydride concept was supported in further studies of austenitic stainless steels and iron–nickel alloys (e.g., [3–8]). Recently [9,10], based on the *ab initio* calculations of interatomic bonds, X-ray diffraction studies of hydrogen-caused crystal lattice dilatation and TEM measurements of stacking fault energy, it was shown that "the γ^* (γ_H) phase" appears from the short-range decomposition in the γ solid solution and, correspondingly, different hydrogen solubility in the submicroscopic areas of different chemical compositions.

A feature of the hydrogen-caused $\gamma \rightarrow \varepsilon_H$ transformation is its occurrence in stable austenitic steels like AISI 310 where no phase transformations are found under any cold work or cooling down to 4.2 K. At the same time, the hydrogen-caused stresses are usually mentioned to be a reason for the $\gamma \rightarrow \varepsilon_H$ transformation [11,12]. This idea is based on the observation [13] that, in its morphology, the hydrogen-induced ε-martensite is not different from that found after cold work or cryogenic treatment. In contrast to this opinion, the *ab initio* calculations of the cohesion energy in Cr–Ni [14] and Cr–Mn [15] austenitic steels led to a conclusion that, in absence of any stresses, hydrogen changes thermodynamic stability of the fcc or hcp phases and, at sufficiently high hydrogen contents, the stability of the hcp phase prevails in Cr–Ni and non-monotonically varies with increasing hydrogen content in Cr–Mn steels.

A practical significance of studies of hydrogen-induced ε-martensite is concerned with the idea that it assists the hydrogen embrittlement of austenitic steels (e.g., [4,16–18]). At the same time, as shown in [19,20], ε_H-martensite does not really affect ductility of austenitic steels at its low amounts, whereas even improves the hydrogen resistance at its higher fractions.

This study is an attempt to shed light on the controversial topic of ε_H martensite origin and its role in hydrogen embrittlement.

2. Experimental

Steels Cr15Ni40, Cr15Ni25 and Cr15Ni25Si2 were melted under argon atmosphere in the arc furnace as ingots of 50 g in the weight. Iron, chromium, nickel and silicon of 99.9% purity were used for melting. These compositions were chosen for studies taking into account that nickel increases and silicon decreases the stacking fault energy in austenitic steels, preventing or assisting

* Corresponding author.
E-mail address: gavr@imp.kiev.ua (V.G. Gavriljuk).

http://dx.doi.org/10.1016/j.msea.2015.09.015
0921-5093/

Table 1
Chemical compositons, mass%.*

Steel	Cr	Ni	Si	Fe
Cr15Ni40	14.71	40.5	-	bal.
Cr15Ni25	14.66	25.8	-	bal.
Cr15Ni25Si2	14.99	25.5	1.85	bal.

* impurity elements are present in usual limits.

herewith the formation of ε-martensite.

After melting, the ingots were cold rolled to the plates of 0.5 mm thickness and annealed at 1100 °C in vacuum. Their chemical compositions are presented in Table 1.

The hydrogen charging was carried at room temperature in 1 N H_2SO_4+125 mg l^{-1} $NaAsO_2$ solution using the platinum anode at current density of 50 mA/cm^2 for 48 h. To prevent uncontrolled hydrogen degassing, just after hydrogen charging, the samples were stored in liquid nitrogen. The hydrogen degassing started after installation of samples in the sample holder of the X-ray diffractometer. Each diffraction pattern has been measured in the course of 22 min of permanent holding. The final pattern was obtained after holding for 24 h when the samples could be conventionally considered as hydrogen-free.

To get the data of the strain-induced phase transformation, the X-ray diffraction was also measured after mechanical tests of hydrogen-charged samples. For comparison, the diffraction was also obtained from the corresponding hydrogen charged samples after their holding at RT for time consistent with that of mechanical testing procedure.

For measurements of X-ray diffraction, Huber diffractometer with one-circle Θ-2Θ goniometer and CuK_α radiation under operating voltage of 30 kV was used. The computer program controlled the angular movement of both goniometer and counter. A graphite monochromator was used at the secondary beam to decrease the noise level. The measurements were carried out with the step of 0.04° within a rather small angle range of 38–54° in order to obtain the diffraction patterns at several stages of hydrogen degassing. The fraction of ε-martensite has been estimated comparing integral intensities of γ- and ε-reflections. The fitting of reflection profiles was performed using the program ProFit of Philips company. After fitting, the hydrogen content in the surface layer of hydrogen-charged steels, i.e. hydrogen/metal ratio H/M, was roughly estimated on the small angle component of the broadened $(111)_\gamma$ reflection.

The crystallographic texture was studied using an automated 3 circle X-ray diffractometer DRON-3M equipped with a texture device. The Schultz reflection method was used. The source of X-rays and the detector were oriented so that a particular value of 2θ was specified and a single Bragg reflection was measured. In the course of measurements, the stage of the cradle is tilted and rotated systematically, so that all angular orientations of the sample were investigated.

The test machine H5K-T produced by Hounsfield company, UK, served for studies of mechanical properties. Hydrogen-caused embrittlement was estimated on the decrease in the relative elongation, $(\delta_0-\delta_H)/\delta_0$, %, where δ_0 and δ_H are its values after annealing and charging, respectively.

3. Results

X-ray diffraction patterns of studied steels after hydrogen charging are presented in Fig. 1. It is seen that hydrogen causes two main effects: (i) the broadening of austenitic X-ray reflections and the shift of their gravity center towards smaller angles, (ii) the

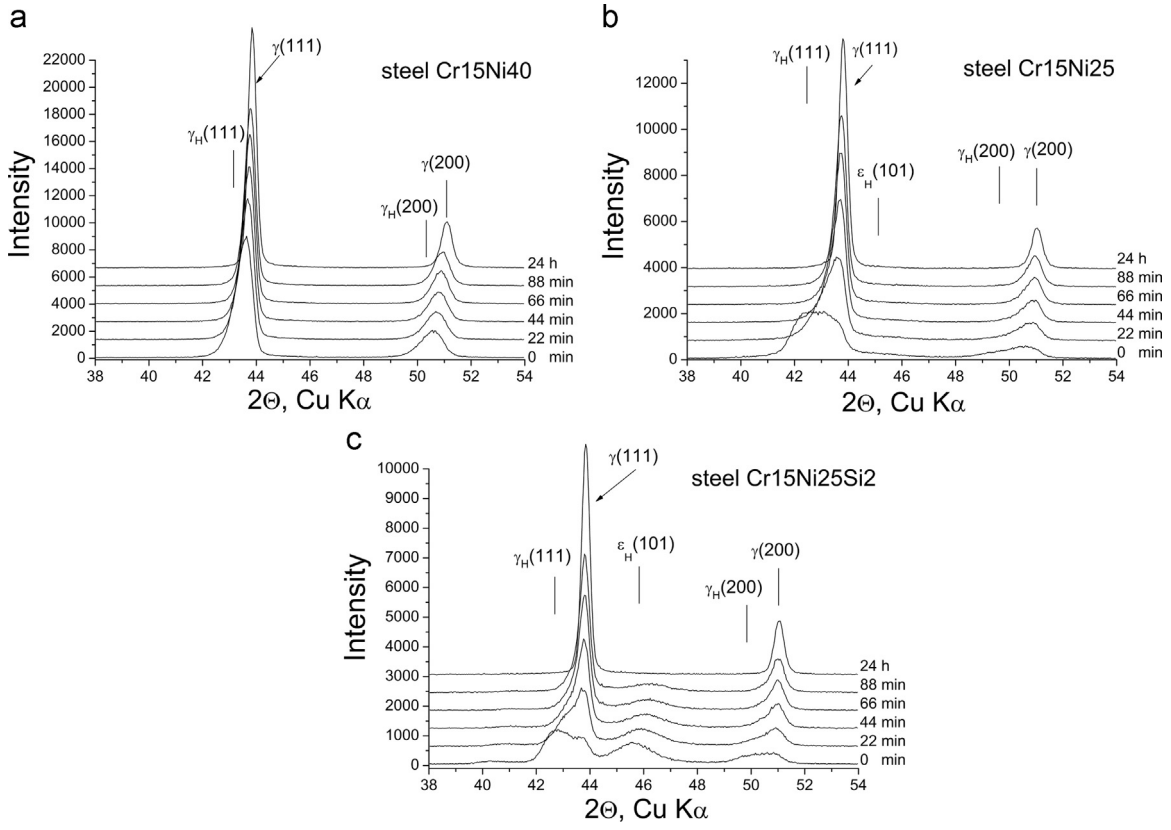

Fig. 1. X-ray diffraction of studied steels after hydrogen charging for 48 h and subsequent degassing at RT: (a) Cr15Ni40, (b) Cr15Ni25, (c) Cr15Ni25Si2. Each diffraction pattern was obtained for subsequent 22 min of sample holding in the diffractometer. The total time of degassing is pointed for each pattern.